J Biomol NMR (2016) 66:187–194
DOI 10.1007/s10858-016-0066-5

ARTICLE

High sensitivity high-resolution full range relaxometry using a fast mechanical sample shuttling device and a cryo-probe

Ching-Yu Chou[1,2,3] · Minglee Chu[6] · Chi-Fon Chang[5] · Tsunai Yu[4] · Tai-huang Huang[4] · Dimitris Sakellariou[1]

Received: 5 July 2016 / Accepted: 29 September 2016 / Published online: 15 October 2016

Abstract Field-dependent NMR studies of bio-molecular systems using a sample shuttling hardware operating on a high-field NMR apparatus have provided valuable structural and dynamic information. We have recently published a design of a compact sample transportation device, called "field-cycler", which was installed in a commercial spectrometer and which provided highly precise positioning and stability during high speed shuttling. In this communication, we demonstrate the first use of a sample shuttling device on a commercial high field standard bore NMR spectrometer, equipped with a commercial triple resonance cryogenically cooled NMR probe. The performance and robustness of the hardware operating in 1D and 2D field cycling experiments, as well as the impact of the sample shuttling time on the signal intensity are discussed.

✉ Tai-huang Huang
bmthh@gate.sinica.edu.tw

Dimitris Sakellariou
dimitrios.sakellariou@cea.fr

1 NIMBE, CEA, CNRS, Université Paris-Saclay, CEA Saclay, 91191 Gif-Sur-Yvette, France

2 Laboratoire des Biomolécules, Département de Chimie, UMR7203 CNRS-UPMC-ENS, Ecole Normale Supérieure, 24 Rue Lhomond, 75005 Paris Cedex 05, France

3 Field Cycling Technology Ltd., 10F., No.136, Chaiqiao Rd., Xiangshan, Hsinchu 300, Taiwan, ROC

4 Institute of Biomedical Science, Academia Sinica, Taipei, Taiwan, ROC

5 Genomics Research Center, Academia Sinica, Taipei, Taiwan, ROC

6 Institute of Physics, Academia Sinica, Taipei, Taiwan, ROC

Keywords Field cycling · Protein dynamics · High-resolution · Relaxometry · Sensitivity · Cryo-probes

Introduction

Nuclear Magnetic Resonance (NMR) studies of biomolecular systems require both high resolution and high sensitivity. Bio-macromolecules, such as proteins and nuclear acids, are usually measured in NMR using concentrations ranging from 10 to 100 μM. Such weak spin concentrations catalyzed the development of cryo-cooled NMR probeheads in order to gain higher sensitivity (Black et al. 1993; Kovacs et al. 2005; Styles et al. 1984) by reducing the noise of the detector electronics. To achieve higher spectral resolution and higher initial polarization, the development of NMR magnets has been pushed to ultra-high magnetic fields, for instance 23.5 T (corresponding to 1 GHz ^{1}H Larmor frequency), or even higher (Yanagisawa et al. 2008). Therefore, very high-field NMR spectrometers equipped with cryo-cooled probes are nowadays essential for acquiring multi-dimensional NMR spectra to be used for biomolecular structural studies (Arthur et al. 2006). Furthermore, NMR relaxation measurements can be used to investigate dynamics information with atomic resolution (Akasaka et al. 1990; Akke et al. 1993; Farrow et al. 1994). Indeed, the magnetic field dependence of spin–lattice (T_1) relaxation times offers invaluable information about spectral density functions, which characterize inter and intra-molecular fluctuations.

Most of the relaxation measurements on macromolecular systems are usually performed at several distinct magnetic field strengths of individual high-field NMR spectrometers. Field-dependent relaxation at low and variable magnetic fields using Fast Field Cycling (FFC)

relaxometry, has been developed for decades (Kimmich and Anoardo 2004; Noack 1986; Nusser and Kimmich 1990), but its application in the investigation of dynamics on biomolecular systems remains restricted because of the lack of chemical shift resolution. Mechanical transportation of the sample between a low field produced by an electromagnet and a high field produced by a superconducting magnet has been used to overcome this limitation. Early sample shuttling experiments used non-conventional NMR probes (Grosse et al. 1999; Swanson and Kennedy 1993; Wagner et al. 1999). In 2003, A. Redfield developed a sample shuttling device which could be used for the first time on a standard high-field NMR spectrometer (Redfield 2003). The sample was first polarized in high field and subsequently shuttled to positions with lower stray field for relaxation. Upon relaxation at low field the sample was then shuttled back to high field for detection with high spectral resolution and sensitivity (Roberts et al. 2004; Roberts and Redfield 2004a, b). This pneumatic shuttling device used the air pressure difference to transport the NMR sample along the central axis of the spectrometer. In order to obtain higher stability, the pneumatic control was later replaced by a mechanical motor driving system and this improved version was used for the study of SARS N-protein dynamics (Clarkson et al. 2009; Redfield 2012). Recently, another pneumatic sample shuttling device, originally designed for Overhauser DNP experiments (Reese et al. 2008), was used to perform field-dependent relaxation studies on a protein sample (3 mM ^{15}N uniformly labeled ubiquitin (UBI) (Charlier et al. 2013)). Meanwhile, a new mechanically-controlled sample shuttling device was published by Chou et al.(Chou et al. 2012). This latter system, named "field-cycler", had a modular design adaptable to various commercial spectrometers and probeheads. The field-cycler was first installed on a standard bore 600 MHz (Bruker AVANCE 600AV) spectrometer, equipped with a 5 mm QXI probehead at the Academia Sinica in Taiwan and recently on a wide bore 500 MHz (Bruker AVANCE II) spectrometer, equipped with a 5 mm homemade probe at CEA in Saclay, France. Since the design of the field-cycler is compatible to the structure of a conventional NMR probehead and to the size of standard sample tubes, it could in principle be used with cryo-cooled NMR probes, to further enhance the sensitivity in biomolecular NMR studies.

In this manuscript, we present the first use of the field-cycler with a high field standard-bore NMR spectrometer equipped with a cryo-probe. We also demonstrate the stability of its operation and evaluate the spectrometer performance and sensitivity enhancement during field cycling experiments. Finally, we study the impact of the sample shuttling time on the signal intensity and we compare the experimental data between two different spectrometers.

Materials and methods

Materials

The biomolecular samples we demonstrated are uniform ^{15}N labeled ubiquitin (UBI) and selective ^{13}C-A,G labeled 14-nt cUUCGg RNA tetra-loop.

Ubiquitin construct was transformed with an expression plasmid (pET-15b) carrying the His-tag coding sequence with thrombin cleavage site under control of the T1 promoter in the BL21(DE3) strain of *E. coli*. To label the protein with ^{15}N, the cells were grown in ^{15}N-M9 medium to an OD of 0.6 and induced with 1 mM IPTG at 30 °C. Cells were harvested by centrifugation and lysed. The protein containing ubiquitin with His-Tag was purified with Ni–NTA affinity chromatography a. The purified protein was dialyzed against buffer (20 mM Tris–HCl and 150 mM NaCl, with pH 8.4) containing thrombin to cleave the His-tag at room temperature for overnight. A second step dialysis against 50 mM KPi buffer at pH 6.0 using a membrane with 3000 dalton molecular weight cutoff was employed to remove the His-tag. Thrombin was further removed using a membrane with 30 K molecular weight cutoff. The purified ubiquitin was concentrated and D_2O was added (10 %) for field-lock.

Selective ^{13}C-A,G labeled 14-nt RNA [5′-PO_4-GGCA-**CUUCG**GUGCC-3′; bold residues constitute the loop)] was synthesized following the protocol published by Thakur et al. (2012). The concentration of the NMR sample was 0.4 mM in 20 mM KH_2PO_4/K_2HPO_4, pH = 6.4, 0.4 mM EDTA and 99 % D_2O.

Hardware

The field-cycler has a modular design that can be easily adapted to various commercial NMR systems. It has been successfully installed on a standard-bore 16.4 T NMR spectrometer (Bruker UltraShield 700 MHz/54 mm AVANCE II) equipped with 5 mm cryo-probe (Bruker 5 mm TCI), on a standard-bore 14.1 T NMR spectrometer (Bruker UltraShield 600 MHz/54 mm AVANCE) equipped with 5 mm QXI probehead, and on a wide-bore 11.7 T NMR spectrometer (Bruker UtraShield 500 MHz/89 mm) equipped with 5 mm homebuilt broadband probe. The length of the railing system (e.g. the length of the guiding rail and the timing belt) can be adjusted to fit the different bore lengths of the magnet cryo-dewars. The details for the construction of the field-cycler can be found in Swanson and Kennedy (1993). Due to longer shuttling distance and the narrow clearance between the NMR tube and RF quartz housing for the cryo-probe of the 700 MHz spectrometer, we placed an additional positioning mechanism on the top

of the railing system, in addition to the original centering flange, to enhance the shuttling precision within the tolerance of the narrow clearance in the probe-head. All the components including the shim-coil were carefully aligned to the center axis of the magnet's dewar.

The stray magnetic field profile of the 16.4 T magnet was measured using the field-cycler as a probe carrier to move a Hall probe (SENIS 3MH3-20T) along the center axis, with a vertical step resolution of 188 µm, set by the field-cycler's motor controller. Comparing the two stray field profiles of the 700 and 600 MHz spectrometers (shown on Fig. 1) we see that the distance from the center of each magnet to the same value of the fringe magnetic field is longer for the 700 MHz NMR system, as expected.

Results

Robustness and performance

The robustness of the field-cycler was tested by shuttling a 5 mm NMR tube in and out of the 5 mm TCI cryo-probe for more than 11,330 times in 24 h. The numbers of repetitions are typical for standard 2D NMR field cycling experiments. We used a sample of RNA (^{13}C-labeled cUUCGg tetraloop) having narrow resonances, in order to evaluate also the shimming stability. 1D ^{1}H spectra were acquired in the beginning (Fig. 2a) and at the end (Fig. 2b) of 24 h continuous high-speed shuttling without any readjustment of shimming currents. The difference spectrum shown on Fig. 2c indicated that the difference after such a long period of shuttling is undetectable. The servo-motor was set to run at 113.04 m/s^2 ($\sim$15.3 g) in constant acceleration/deceleration mode for 53.5 ms for a total trajectory of 57.88 cm. The sample starts and stops smoothly inside the cryo-probe with no wobbling. The sample tube and the cryo-probe didn't show any signs of wear, or other adverse effect for this test, and all subsequent experiments.

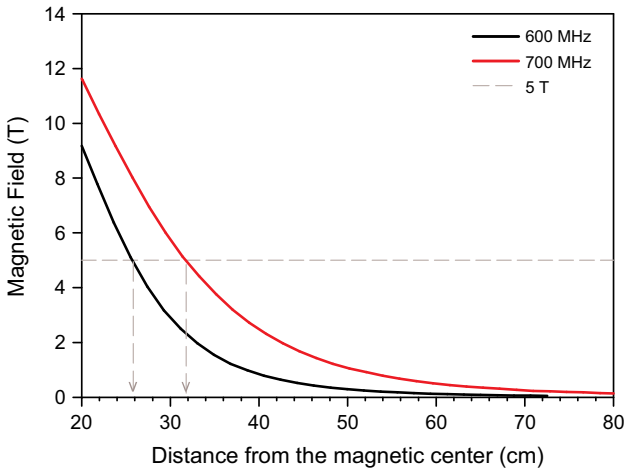

Fig. 1 The stray magnetic fields profiles of Bruker UltraShield 600 MHz (*black line*) and Bruker UltraShield 700 MHz (*red line*) magnets. The Hall probe's position was controlled by the field-cycler to measure both magnetic field profiles at a spatial resolution of 188 µm. It is evident that the distance between the center of the magnet and a given stray field is longer for the 700 MHz spectrometer magnet than that for the 600 MHz apparatus (32 vs. 26 cm at 5 T as specified by the grey dashed lines at 5 T)

To evaluate the performance on biomolecular applications, we compare data recorded of a uniformly ^{15}N-labeled UBI in H_2O:D_2O 9:1 v/v on two liquid-state NMR spectrometers: (1) at 600 MHz with a RT QXI probe, and (2) at 700 MHz with a 5 mm CP TCI cryo-probe. The spectrum shown in Fig. 3a is the ^{1}H–^{15}N HSQC type spin–lattice relaxation (R_1) spectrum of 500 µM UBI sample acquired at 700 MHz spectrometer in 20 min with sample shuttling between 16.4 and 1.0 T, separated by a distance of 49.59 cm. The sample stayed at 1.0 T during the relaxation delay time of 0.048 s. A standard pulse sequence with WATERGATE solvent suppression module was used. In Fig. 3b, we compare the signal intensities of the corresponding stripes of ^{1}H–^{15}N HSQC spectra (along the ^{1}H dimension) obtained with 800 µM sample at 600 MHz (red) and 500 µM at 700 MHz (black), respectively. Both spectra had the same spectral resolution. 128 t_1 increments were recorded each being a sum of 2 scans using the method of States-TPPI for phase sensitive 2D detection. 2048 points were recorded in the direct dimension and no zero filling was applied prior to 2D FT. The repetition delays were 3 s while the relaxation delay was equal to 48 ms. The acquisition time was about 25 min per spectrum. The superior signal sensitivity at 700 MHz is evident, even though the sample used at 700 MHz is less concentrated.

Discussion

Comparison of pneumatic and mechanical design

Redfield's device, as well as the field-cycler, are both compatible with existing commercial spectrometers and probeheads (Chou et al. 2012; Redfield 2012). Both of these systems use 5 mm tubes, commonly used in most biomolecular NMR studies, accept the same sample volumes (typically 200–300 µl or even higher) and benefit the intrinsic sensitivity of the instrument as in its standard operation. Moreover, the field-cycler uses tubes with conventional length while Redfield's device requires them to have a special length. This is significant since the filling factor from both systems is identical to that of conventional non-shuttling experiments. On the other hand, pneumatic systems other than that of Redfield's device often use

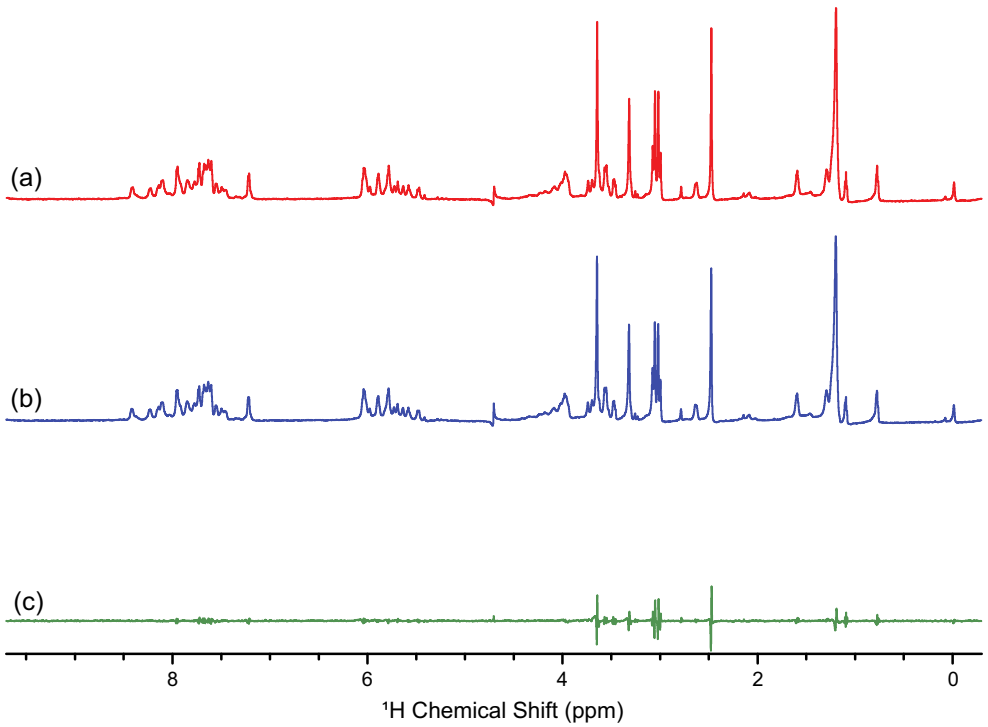

Fig. 2 Spectrum stability test after 11 k times of sample shuttling between 16.4 T (i.e. the center of the 700 MHz spectrometer magnet) and 0.5 T. 1D ^{1}H spectra of 0.4 mM ^{13}C labeled cUUCGg tetraloop in 20 mM $KHPO_4$, pH 6.4, 0.4 mM EDTA and 99 % D_2O are presented. **a** Spectrum before sample shuttling; **b** Spectrum after ~11 k times of fast (53.5 ms shuttling time) shuttling in 24 h. **c** Difference spectrum (**a**)–(**b**) demonstrating that shuttling does not influence the spectral quality

restricted volume sample holders (for instance, a recently published relaxometry study (Charlier et al. 2013) using a pneumatic shuttling reported sample volumes of only 60 µl), having thus reduced filling factors and leading to massive reductions in signal sensitivity.

In addition to spectrometer adaptation and compatibility, the time stability of operation is a serious concern in field-cycling biomolecular NMR studies. Most experiments require long experimental times due to the low sensitivity, coming either from the low sample concentration, or the structural condition of the bio-samples. We have previously constructed a pneumatically controlled shuttling system based on Redfield's design that uses differential air pressure to move the sample rapidly. High-pressure air is capable of generating sudden and strong forces to push the sample carrier. It is also, however, not easily controllable and does not produce a constant force in time. An optimal air control unit requires large buffer gas behind all control valves to produce a stable and constant force to push the shuttle (Redfield 2003). Since the compressed air can only generate uni-directional force, the stopping mechanism is also a critical design component. Nowadays, the most common design is to have one or two stop tubes/rods and use the force from collision to stop the sample, either at the locations of stray field or inside the probehead (Krahn et al. 2010; Redfield 2003; Reese et al. 2008). This collision mechanism generates sudden decelerations on the sample, which can cause mechanical instabilities on the shuttling motion and might increase the risk of sample aggregation/precipitation during the field-cycling experiments. Thus, for high stability sample shuttling, a mechanical motion control can provide a much more stable force, since the trajectory can be programmed and the stopping mechanism can be extremely smooth without hard collisions (Chou et al. 2012; Redfield 2012). Moreover, the field-cycler has a shorter shuttle sample holder to overcome the vibration problem (Chou et al. 2012; Redfield 2012). The field-cycler can achieve the same shuttling time as most pneumatic control systems, while keeping the high stability for long time operation. Finally, the field-cycler requires only 30 ms equilibration time after high-speed shuttling before signal detection whilst the pneumatic control systems require longer equilibration time due to the strong collision. Consequently, the total sample transportation time for the field cycler is, in fact, shorter than the pneumatic control systems.

Quantitative comparison of shuttling performance on different spectrometers

The sensitivity comparison of the field-cycler at different spectrometers equipped with different probeheads is very informative to identify critical design parameters. Here we

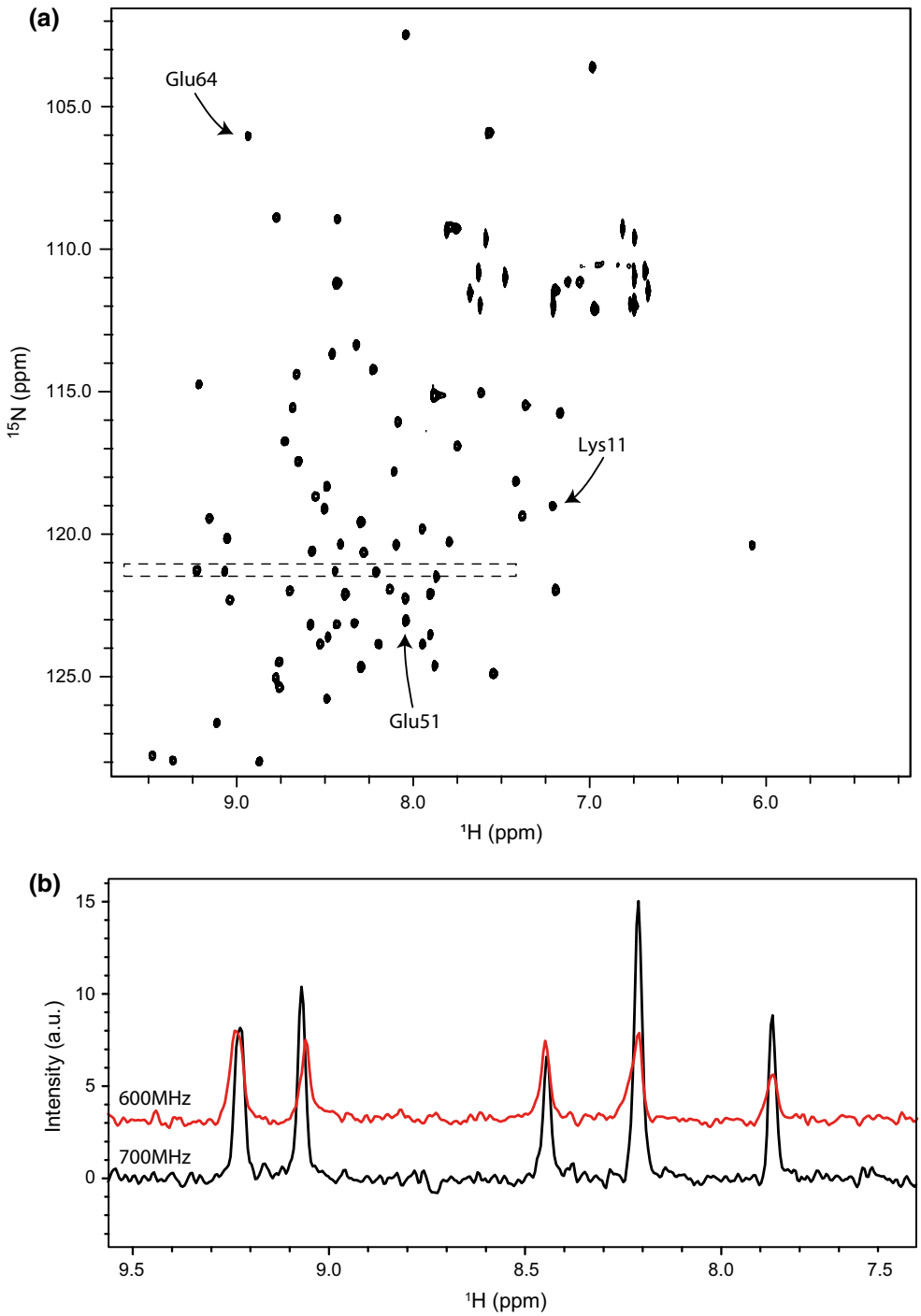

Fig. 3 **a** ^{15}N–^{1}H HSQC 700 MHz spectrum from R_1 measurements of 500 μM ^{15}N-UBI sample, acquired in 20 min under field cycling from 16.5 to 1.0 T with the relaxation delay time of 48 ms. The used probehead was a 5 mm TCI Bruker cryo-probe. The resonance enclosed by the *dashed square* is the peak for calculating the ratio of SNR between two hardware configurations: Bruker UltraShield 700 MHz/TCI cryo-probe and 600 MHz/QXI RT probe. **b** ^{1}H slices at 121.3 ppm ^{15}N chemical shift corresponding to the *long dashed rectangle* area of the previous 2D spectrum are displayed in the lower slice. The *red slice* is extracted from 1.0 T R_1 measurement acquired at 600 MHz, and the black is extracted from the same shuttling experiment at 700 MHz

will compare the signal to noise ratio of two series of ^{1}H–^{15}N HSQC R_1 spectra acquired in field-cycling mode on two spectrometers, at 700 MHz equipped with a cryo-probe and at 600 MHz equipped with a room temperature probe. We will see that field-cycler hardware setup does not perturb the native SNR enhancement originating from

the use of the cryo-probe. However, the SNR of field-cycling experiments is affected by the shuttling time and the length of relaxation time. All these effects are included in the experimental measurements of SNR in field-cycled R_1 ^1H–^{15}N HSQC spectra with identical relaxation delays.

To gain better understanding we separate the ratio of the SNR into two terms, λ and g:

$$\frac{SNR[600\,\mathrm{MHz}]}{SNR[700\,\mathrm{MHz}]} = \lambda \cdot g \tag{1}$$

The factor g accounts for the intrinsic difference in field strengths and spectrometer performance (RT probe, or cryo-cooled probe and preamplifier electronics, etc.), as well as for the number of scans and the concentrations of the sample. Experimentally, we compared resonance by resonance in two spectra acquired at 600 MHz and 700 MHz. The selected resonances here are Glu64, Lys11, and Glu51. The N–H resonance of Glu64 has been evaluated from the SNR comparison of standard ^1H–^{15}N HSQC spectra on uniform ^{15}N labeled ubiquitin and found to be 0.3125 times lower at 600 MHz with RT-probe than that obtained at 700 MHz with cryo-probe, therefore g = 0.3125. Besides the spectrometer setup, g is also influenced by spin–spin relaxation.

The factor λ is equal to 1 in non-shuttling experiments, and in shuttling experiments it accounts for signal loss during shuttling due to spatially dependent relaxation rates. It thus depends of the shuttling distance, the velocity profile, the stray field profile of the spectrometer, as well as the dispersion curve of the T_1 time of the sample. To measure λ, we collected the ^1H–^{15}N HSQC type R_1 experiments by field-cycling the sample to the following stray magnetic field strengths: 7, 5, 4, 3, 2.1, 1 T with identical repetition times at both spectrometers. Indeed, shuttling time directly depends on the stray field profiles of the spectrometers as can be seen on Fig. 4. The relationship between the shuttling time (Δt) and the measured parameter (in our case the spin–lattice relaxation time T_1) is crucial: the ratio between Δt and the T_1 influences the observed SNR and preferably $\Delta t \leq T_1$ for better SNR. To account for all effects the signal intensity can be written as:

$$I(t;\omega_{FC}) = I(0;\omega) \times \delta_{up}[\Delta t(\omega_{HF});\omega_{FC}] \times e^{-\frac{t}{T_1(\omega_{FC})}} \times \delta_{down}[\Delta t(\omega_{HF});\omega_{FC}] \tag{2}$$

where Δt is the sample shuttling time, the field-cycling stray field is ω_{FC}, the highest Larmor frequency is ω_{HF}, the delay time during the relaxation period in the measurement is presented as t. The spin–lattice relaxation time T_1 at ω_{FC} is labeled as $T_1(\omega_{FC})$. And, the factors perturbed by shuttling are approximated as:

$$\delta_{up}[\Delta t(\omega_{HF});\omega_{FC}] = \int_{\omega_{HF}}^{\omega_{FC}} \int_{0}^{\Delta t} \exp(-dt/T_1(\omega))dtd\omega,$$

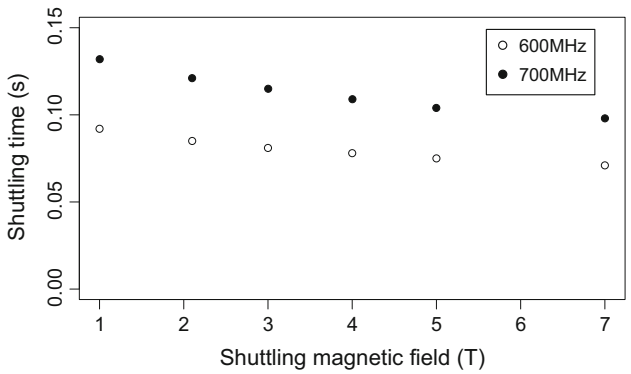

Fig. 4 Stray field-dependent shuttling time plot for the Bruker UltraShield 600 MHz (*open circles*), and for the Bruker UltraShield 700 MHz (*filled circles*) NMR spectrometers. The shuttling time difference for the same stray magnetic fields is due to the different stray field profiles of the superconducting magnets

$$\delta_{down}[\Delta t(\omega_{HF});\omega_{FC}] = \int_{\omega_{FC}}^{\omega_{HF}} \int_{0}^{\Delta t} \exp(-dt/T_1(\omega))dtd\omega$$

$\Delta t(\omega_{HF})$ is the same for shuttling up and down ($\delta_{up} = \delta_{down} = \delta$). The $T_1(\omega)$ profile is unknown during the whole shuttling procedure because $T_1(\omega)$ is our target function of field-cycling experiments.

The g factor accounts for the ratio of$I(0;\omega)e^{-\frac{t}{T_1(\omega_{FC})}}$ obtained at 600 and 700 MHz while the $\delta_{up}[\Delta t(\omega_{HF});\omega_{FC}]$ and $\delta_{down}[\Delta t(\omega_{HF});\omega_{FC}]$ terms are related to λ as:

$$\lambda \sim \frac{\delta_{up}(600\,\mathrm{MHz})\delta_{down}(600\,\mathrm{MHz})}{\delta_{up}(700\,\mathrm{MHz})\delta_{down}(700\,\mathrm{MHz})} \tag{3}$$

$\delta_{up}(600\,\mathrm{MHz})$, $\delta_{down}(600\,\mathrm{MHz})$ and $\delta_{up}(700\,\mathrm{MHz})$, $\delta_{down}(700\,\mathrm{MHz})$ are the signal losses caused by the relaxation profile in the stray field during the shuttling time in different spectrometers, 600 MHz and 700 MHz, respectively.

The λ is calculated directly from the ratio of SNR on the selected peaks shown in Fig. 2 and divided by the impact from the spectrometer setup, which is the value extracted by comparing two non-field-cycling HSQC spectra (i.e. g = 0.3125 at Glu64, g = 0.451 at Lys11, and g = 0.2106 at Glu51).

The λ ratio indicates the loss due to different stay magnetic profile and the shuttling time, which is presented in Fig. 5. For example, the sample travelling distance for field-cycling to 5 T for the 700 MHz spectrometer is 1.23 times that of the 600 MHz spectrometer, leading to a 60 % increase in shuttling time for the 700 MHz (Δt is 104 ms) as compared to that for the 600 MHz (Δt is 65 ms). Nonetheless, for the peak-1, the SNR at 700 MHz is still 2.54 higher than at 600 MHz. Thus, $\frac{SNR(600\,\mathrm{MHz})}{SNR(700\,\mathrm{MHz})} = 0.394$,

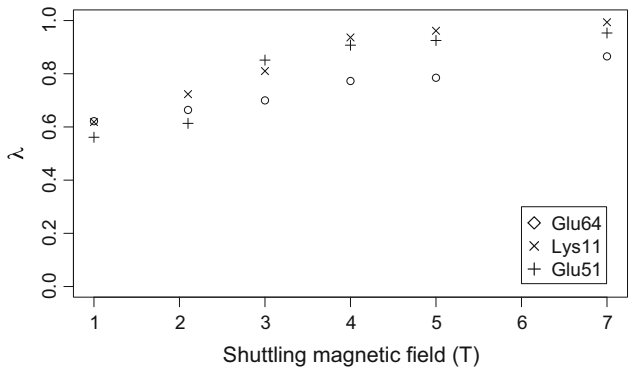

Fig. 5 The experimentally measured stray field-dependent λ factor (see Eq. 1) extracted from the three ^{15}N resonances as selected in Fig. 3a. This factor accounts for the signal loss due to shuttling and is influenced by the sample shuttling time and the stray field profile of the host spectrometer

corresponding to $\lambda = 1.2$, which is 20 % higher than the non-shuttling ratio of 0.3125, for which $\lambda = 1$. This signal loss is highly compensated by the sensitivity enhancement due to the cryo-probe and the higher magnetic field during the polarization and acquisition periods.

The overall signal sensitivity in shuttling experiments depends thus on the spatial profile of the stray magnetic field and the field strength of the NMR magnet. This means that the field-cycler in different spectrometers will have different sample shuttling times for the same field-cycling magnetic field. Strongly shielded standard-bore magnets will be optimal in terms of shuttling times because of the shorter travelling distances. Accordingly, the signal to noise ratio of a field-cycling experiment as well as the range of measurable NMR parameters will depend on the design and field strength of the magnet.

Conclusion

We have performed the first high-resolution field-cycling NMR experiments using a mechanical sample-shuttling device, the field-cycler, and a commercial cryo-cooled probe. This combination provides ultra-high sensitivity and spectral resolution in relaxometry experiments over the full field range, without any negative impact on the spectrometer performance and safety. This extends the measurable systems to diluted proteins and even to protein systems having less chemical shift dispersion, e.g. intrinsically disordered systems. We have also performed a quantitative analysis on the impact of the stray field profile on the signal to noise ratio. In addition to the wide adaptation on various spectrometers, the presented field-cycler has the potential to be used inside superconducting NMR magnets having multiple homogeneous spots (Chou et al. 2015) combined with radio-frequency coils, and allow for correlation experiments benefiting from the low magnetic field for easier spin manipulations (e.g. spin lock or broadband excitation, etc.) or for exchange. The adaptation to a *dual-field NMR* system is currently in progress in our laboratory.

Acknowledgments We greatly acknowledge Dr. Sophie Zinn-Justin (CEA) for stimulating discussions and for allowing us access to the 700 MHz spectrometer, Dr. Nikolas Birlirakis (ENS) for useful comments on the manuscript and Dr. F. Ferrage (ENS) for comments and suggestions. We would like to give the special acknowledgement to Dr. Jan Marchant and the labs of Prof. Michael F. Summers and Prof. Kwaku T. Dayie in Maryland University, USA, for the UUCG tetra-loop RNA sample preparation. We also thank Mr. Angelo Guiga and the staffs in the Academia Sinica Machine Shop, Taiwan, especially Mr. Cherng-Yin Lin, for the production of the high-precision hardware. This work is supported by ERC grants 2F4BIODYN and R-EVOLUTION-M-R (StG 205119), ANR DYN-IDP in France, and NSC 102-2113-M-001-010 from The National Science Council, The Republic of China.

References

Akasaka K, Ishima R, Shibata S (1990) Proton spin relaxation in biopolymers at high magnetic fields. Phys B Condens Matter 164:163–179

Akke M, Skelton NJ, Kordel J, Palmer AG, Chazin WJ (1993) Effects of ion binding on the backbone dynamics of calbindin D9 k determined by nitrogen-15 NMR relaxation. Biochemistry 32:9832–9844

Arthur G, Palmer WJF III, Cavanagh John, Sketon Nicholas J, Rance Mark (2006) Protein NMR spectroscopy: principles and practice, 2nd edn. Academic Press Inc, Cambridge

Black RD, Early TA, Roemer PB, Mueller OM, Mogrocampero A, Turner LG, Johnson GA (1993) A high-temperature superconducting receiver for nuclear-magnetic-resonance microscopy. Science 259:793–795

Charlier C et al (2013) Nanosecond time scale motions in proteins revealed by high-resolution NMR relaxometry. J Am Chem Soc 135:18665–18672

Chou CY, Chu M, Chang CF, Huang TH (2012) A compact high-speed mechanical sample shuttle for field-dependent high-resolution solution NMR. J Magn Reson 214:302–308

Chou C-Y, Ferrage F, Aubert G, Sakellariou D (2015) Simple method for the generation of multiple homogeneous field volumes inside the bore of superconducting magnets. Sci Rep 5:12200

Clarkson MW, Lei M, Eisenmesser EZ, Labeikovsky W, Redfield A, Kern D (2009) Mesodynamics in the SARS nucleocapsid measured by NMR field cycling. J Biomol NMR 45:217–225

Farrow NA et al (1994) Backbone dynamics of a free and a phosphopeptide-complexed Src homology 2 domain studied by 15 N NMR relaxation. Biochemistry 33:5984–6003

Grosse S, Gubaydullin F, Scheelken H, Vieth HM, Yurkovskaya AV (1999) Field cycling by fast NMR probe transfer: design and application in field-dependent CIDNP experiments. Appl Magn Reson 17:211–225

Kimmich R, Anoardo E (2004) Field-cycling NMR relaxometry. Prog Nucl Magn Reson Spectrosc 44:257–320

Kovacs H, Moskau D, Spraul M (2005) Cryogenically cooled probes—a leap in NMR technology. Prog Nucl Magn Reson Spectrosc 46:131–155

Krahn A et al (2010) Shuttle DNP spectrometer with a two-center magnet. Phys Chem Chem Phys 12:5830–5840

Noack F (1986) NMR field-cycling spectroscopy—Principles and applications. Prog Nucl Magn Reson Spectrosc 18:171–276

Nusser W, Kimmich R (1990) Protein backbone fluctuations and NMR field-cycling relaxation spectroscopy. J Phys Chem-Us 94:5637–5639

Redfield AG (2003) Shuttling device for high-resolution measurements of relaxation and related phenomena in solution at low field, using a shared commercial 500 MHz NMR instrument. Magn Reson Chem 41:753–768

Redfield A (2012) High-resolution NMR field-cycling device for full-range relaxation and structural studies of biopolymers on a shared commercial instrument. J Biomol NMR 52:159–177

Reese M et al (2008) Construction of a liquid-state NMR DNP shuttle spectrometer: first experimental results and evaluation of optimal performance characteristics. Appl Magn Reson 34:301–311

Roberts MF, Redfield AG (2004a) High-resolution P-31 field cycling NMR as a probe of phospholipid dynamics. J Am Chem Soc 126:13765–13777

Roberts MF, Redfield AG (2004b) Phospholipid bilayer surface configuration probed quantitatively by P-31 field-cycling NMR. Proc Natl Acad Sci USA 101:17066–17071

Roberts MF, Cui Q, Turner CJ, Case DA, Redfield AG (2004) High-resolution field-cycling NMR studies of a DNA octamer as a probe of phosphodiester dynamics and comparison with computer simulation. Biochemistry 43:3637–3650

Styles P, Soffe NF, Scott CA, Crag DA, Row F, White DJ, and White PCJ (1984) A high-resolution NMR probe in which the coil and preamplifier are cooled with liquid helium. J Magn Reson 60:397–404

Swanson SD, Kennedy SD (1993) A sample-shuttle nuclear-magnetic-relaxation-dispersion spectrometer. J Magn Reson Ser A 102:375–377

Thakur CS, Luo Y, Chen B, Eldho NV, Dayie TK (2012) Biomass production of site selective 13C/15 N nucleotides using wild type and a transketolase *E. coli* mutant for labeling RNA for high resolution NMR. J Biomol NMR 52:103–114

Wagner S, Dinesen TR, Rayner T, Bryant RG (1999) High-resolution magnetic relaxation dispersion measurements of solute spin probes using a dual-magnet system. J Magn Reson 140:172–178

Yanagisawa Y et al (2008) Towards beyond-1 GHz solution NMR: internal 2H lock operation in an external current mode. J Magn Reson 192:329–337